19th Brazilian Congress of Thermal Sciences and Engineering
November 06th-10th, 2022, Bento Gonçalves - RS - Brazil

ENC-2022-0100
NUMERICAL STUDY OF TANDEM SLENDER CYLINDERS ON A TURBULENT CROSSFLOW

Patrick Batista Habowski
Universidade Federal do Rio Grande do Sul, Programa de Pós-Graduação em Engenharia Mecânica (PROMEC), Rua Sarmento Leite, 425, Porto Alegre, CEP 90050-170, Brazil.
patrick.habowski@ufrgs.br

Roberta Fátima Neumeister
Universidade Regional Integrada do Alto Uruguai e das Missões, Avenida Sete de Setembro, 1621, Erechim-RS, CEP 99709-910, Brazil.
robertaneumeister@uricer.edu.br

Adriane Prisco Petry
Universidade Federal do Rio Grande do Sul, Programa de Pós-Graduação em Engenharia Mecânica (PROMEC), Rua Sarmento Leite, 425, Porto Alegre, CEP 90050-170, Brazil.
adrianep@mecanica.ufrgs.br

Sérgio Viçosa Möller
Universidade Federal do Rio Grande do Sul, Programa de Pós-Graduação em Engenharia Mecânica (PROMEC), Rua Sarmento Leite, 425, Porto Alegre, CEP 90050-170, Brazil.
svmoller@ufrgs.br

Abstract. *This article presents a numerical study of a pair of fixed slender circular cylinders tandem placed to a turbulent crossflow. Spacing ratios (T/D) of 5, 7.5, and 10 were tested, where T is the horizontal distance between the cylinders with diameter D. The Reynolds number of the experiment was set as 6.67×10^3, computed for the cylinder diameter of 10 mm. Flow patterns, force coefficients, Strouhal number, and velocity fields were compared with literature numerical and experimental results. The setup with the fixed cylinders was computed employing the OpenFOAM software, and the mesh was generated by the gmsh open software. The conservation equations were solved by LES simulation with the k-dynamic turbulence model. The main results showed that the higher the T/D spacing ratio, the lower the mean flow velocity behind the downstream cylinder. On the other hand, an increase in the velocity fluctuations was observed with the increase of the T/D spacing ratio. Strouhal numbers obtained in this study presented a fixed value of 0.195, independent of the T/D spacing ratios. Flow visualization presented vortex reattachment in all the tested cases.*

Keywords: *Computational Fluid Dynamics (CFD), Flow-Induced Vibrations, Slender Cylinders, Turbulent Flow, Vortex Shedding.*

1. INTRODUCTION

Circular cylinders are a classical field of study in fluid mechanics since these structures are used to explore simplified arrangements of more complex flow patterns, such as the flows around heat exchangers, nuclear reactors, buildings, chimneys, bridges pillars, and others (Alam et al., 2003; Alam and Sakamoto, 2005; Habowski et al., 2019). If a circular cylinder is placed in a turbulent crossflow, a wake downstream the cylinders is formed, disturbing the pressure field nearby. This disturbance can lead to structural vibrations, known as FIV (Flow-Induced Vibrations). If the energy present in the flow is enough, the structure itself may suffer damage due to the generated vibration. The structure can also oscillate (Habowski et al., 2020b) or even rotate (Habowski et al., 2022), depending on the flow and the setup conditions.

In the literature, flow past cylinders and cylinder arrangements are widely discussed. Zdravkovich (1987) studied the interference in arrangements with circular cylinders placed in tandem, side-by-side and staggered positions. The author classified the observed phenomenon according to the flow regime, cylinder alignment, and T/D ratios, where T is the distance between cylinder centers and D is the cylinder diameter. The author described the vortex shedding, drag and lift coefficients, Strouhal number, and wake interference for the studied cases. Sumner et al. (2000) explored the flow visualization employing PIV (Particle Image Velocimetry) for configurations with two circular cylinders of equal

diameter. Nine flow patterns were identified and were observed processes as shear layer reattachment, vortex pairing and synchronization, induced separation, and vortex impingement. The author also observed that the two shear layers of the downstream cylinder have different frequencies of vortex shedding.

There is no doubt that the flow around circular cylinders is complex. Sumner (2010) and Zhou and Alam (2016) presented an extensive review of the numerical and experimental results involving the flow around cylinders. Both authors summarized the results for the Strouhal number, fluid forces and coefficients, heat and momentum transport, and Reynolds number effects. The wake interference between the cylinders is described, and in configurations with circular cylinders tandem placed, the T/D spacing ratio is a parameter that influences the vortex shedding patterns in the downstream cylinder. Besides the T/D ratio, factors such as the Reynolds number and cylinders angle to the flow also influence the vortex shedding patterns.

The vortex shedding from the upstream cylinder may induce the downstream cylinder to vibrate at different frequencies or amplitude. This phenomenon (FIV) is reported by Kim et al. (2009) in configurations with cylinders tandem placed to the flow, considering that both cylinders or only one are free-to-vibrate. The authors were able to identify vibration regimes as the T/D was varied. Yao and Jaiman (2019) presented a study of the stability of WIV (Wake Induced Vibrations) modes of two circular cylinders in a tandem arrangement. The main results emphasized that the critical Reynolds number reduces as the T/D ratio is increased.

Previous studies performed by Igarashi (1981) in a pair of circular cylinders tandem placed to the flow showed that for configurations with $T/D > 3$, the shear layers begin to roll up in the wake, and a fully developed vortex street is formed behind the upstream cylinder. More recently, Alam et al. (2003) explored experiments with two circular cylinders in tandem arrangements for several T/D at a subcritical Reynolds number of 6.5×10^4. The authors were able to systematize drag, lift and pressure coefficients and their fluctuations, reattachment position of the shear layers, and Strouhal numbers. From the results observations, it was concluded that the fluctuating drag and lift forces are very sensitive to the T/D ratio. It was also observed that these fluctuating fluid forces interfere with the shear layer reattachment in the downstream cylinder.

In the numerical study with experimental support made by Neumeister et al. (2018), the flow around two circular cylinders was analyzed using URANS (Unsteady Reynolds Averaged Navier-Stokes) simulations with $k\omega$–SST–SAS (Shear Stress Tensor – Scale Adaptive Simulation) turbulence model. Through the velocity data monitored at specific points in the domain, it was possible to corroborate the numeric results with experimental data obtained from an aerodynamic channel. Derakhshandeh et al. (2014) compared the $k\omega$–SST and $k\omega$–SST–SAS models in a VIV (Vortex Induced Vibration) analysis for the flow around two circular cylinders. Comparing both models with experimental results, the $k\omega$–SST–SAS model presented a better performance. The same $k\omega$–SST–SAS turbulence model was employed in the study of Zhao et al (2011) with wavy cylinders, presenting good accordance with experimental drag and lift coefficients. Palau-Salvador et al. (2008) studied the flow around two finite cylinders in tandem position using LES simulation. The authors compared the obtained results with experimental PIV results from the literature and observed good accordance, but differences were identified in the flow in the gap between the cylinders.

In our laboratory, several numerical and experimental studies involving flow past cylinders and cylinders arrays were carried out. Neumeister et al. (2022) studied the wake-induced vibration in tandem circular cylinders, exploring experiments in both aerodynamic and hydrodynamic channels for T/D ratios ranged 2.5 to 10. The setup in the aerodynamic channel was mounted with the upstream cylinder fixed and the downstream cylinder free-to-vibrate transversally to the flow. Flow visualization was obtained from the hydrodynamic flow channel, where both cylinders were rigidly mounted. The authors emphasized the influence of the wake from the upstream cylinder on the vibration regime and lift forces in the second cylinder. Influences on acceleration in the transverse direction of the downstream cylinder due to the upstream vortex shedding were perceived in all T/D ratios studied.

Habowski et al. (2020b) presented flow visualizations in a setup with two circular cylinders placed at several angles to the flow, from side-by-side to tandem configurations for a P/D ratio of 1.26, being P the distance between the cylinder's centers. Neumeister et al. (2021) performed experiments to describe the FIV interaction in the subcritical flow regime for a single cylinder and pairs of cylinders in tandem and side-by-side arrangements with a P/D ratio of 1.26. The authors performed 25 experiments varying the damping and mass ratios of the cylinders and observed a sudden increase in the amplitude of the transversal oscillations for the configuration where both cylinders were free-to-vibrate.

Following the observations performed by Neumeister et al. (2021), Habowski et al. (2020a) developed an experiment using a setup where two circular cylinders were set on a circular table and placed inside a wind tunnel. The upstream cylinder was aligned with the center line of the circular table, and the downstream cylinder was eccentrically placed. The free flow was accelerated close to the cylinders by throat-like devices to force the cylinders to oscillate even for low free flow velocities. The authors reported a proportional relation between the Reynolds number and the amplitude of the oscillations.

The present study aims to investigate the wake flow patterns, force coefficients, and Strouhal number of a pair of fixed circular slender cylinders tandem placed inside an aerodynamic channel, with a Reynolds number of 6.67×10^3, using LES simulation. Spacing ratios T/D of 5, 7.5, and 10 were studied. The blockage ratio of the experiment is 1%, considering the cylinder diameter of 10 mm and the width of the aerodynamic channel of 1000 mm (Fig. 1).

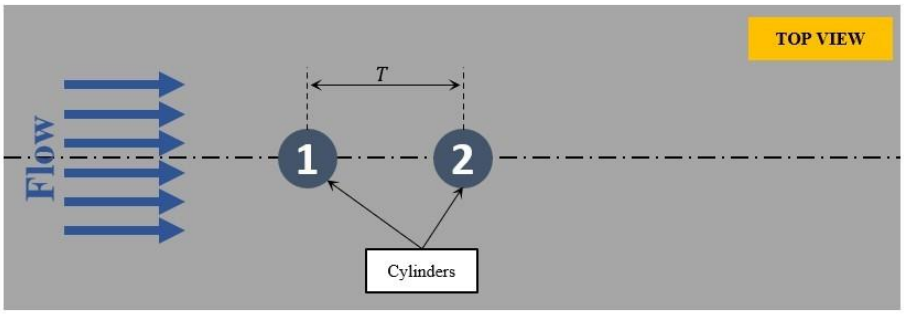

Figure 1. Schematic geometry of the present study.

2. NUMERICAL METHODOLOGY

The solution of the conservation equations was performed by FVM (Finite Volume Method), where the three-dimensional equations of mass and transport momentum were solved by the OpenFOAM-v9 open-source software using the LES dynamic model. According to Wilcox (2006), in the LES modeling, the turbulent fluctuations are averaged only over part of their spectrum. It is defined that the large scales are directly affected by the domain and the boundary conditions and need to be calculated. Small scales can be considered isotropic and have universal characteristics, being more easily to be modeled. In this model, the incompressible mass conservation and Navier-Stokes equations are filtered by a process of scale separation using a spatial filter Δ (Neto, 2002), resulting in the filtered LES equations (Eq. 1 and Eq. 2, respectively).

$$\frac{\partial \overline{u_i}}{\partial x_i} = 0 \tag{1}$$

$$\frac{\partial \overline{u_i}}{\partial t} + \overline{u_j}\frac{\partial \overline{u_i}}{\partial x_j} = -\frac{1}{\rho}\frac{\partial \bar{p}}{\partial x_i} + \nu\frac{\partial^2 \overline{u_i}}{\partial x_j \partial x_j} - \frac{\partial \tau_{ij}}{\partial x_i} \tag{2}$$

where $\bar{u}$ is the filtered solved velocity field and the sub-grid stress tensor τ_{ij} is defined as $\tau_{ij} = \overline{u_i u_j} - \overline{u_i}\,\overline{u_j}$. For the LES dynamic model, the coefficients of the turbulence kinetic energy equation are derived from local flow properties instead of being fixed values as used in the classical LES model (Kim and Menon, 1995).

As the large scales of the flow are solved in the LES modeling, the results obtained are dependent on the mesh refinement. Considering this, it is very important to evaluate the mesh quality before running the simulations. One practical mesh quality analysis consists of measuring the amount of the turbulence kinetic energy being resolved due to the mesh refinement and comparing with the amount of the turbulence kinetic energy being modeled, the so-called k_{index}. According to the literature works (McDermott et al., 2010; Pope, 2004), good results are obtained as long as the ratio between the resolved and the total turbulent kinetic energy is higher than 80% (Eq. 3).

$$k_{index} = \frac{k_{resolved}}{k_{total}} > 80\% \tag{3}$$

In this work, the numerical flow domain is defined based on the *Debi Pada Sadu* wind tunnel of the LMF (Fluid Mechanics Laboratory) of UFRGS (*Universidade Federal do Rio Grande do Sul*). The original dimension of the wind tunnel is a rectangular channel of 1 m × 1 m (height × width) with a length of 5.7 m. As the blockage ratio is equal to 1%, the wall effects were neglected. Thus, the numeric domain was restricted to a bounding box measuring 450 mm × 200 mm × 30 mm in x, y, and z directions, respectively. The upstream cylinder was positioned 10 times the diameter length far from the inlet wall.

The mesh generation was performed by the gmsh open-source software, which has an interface with the OpenFOAM software. As the geometry of the domain and the object of study are simple, a structured mesh could be created. The region close to the cylinders, which is the region of interest in this study, was refined by dividing the edges of the cylinder into 56 parts, generating a mesh with 230,160 volumes. An isometric view of the mesh is presented in Fig 2a, and a region close to the cylinders is presented in Fig. 2b.

The boundary conditions were defined by prescribed velocity and pressure fields. At the entrance, the x-flow velocity component of 10 m/s was set with a turbulence intensity of 1%, and the velocities in the y- and z-axes were set as zero (Fig. 2c, detail "I"). Also, the initial internal velocity field was set as zero. In the sidewalls, the slip condition was adopted, since the wall effects were neglected (Fig. 2c, details "S"), and both upstream and downstream cylinder walls were set as

no-slip condition (Fig. 2c, detail "C"). The prescribed pressures at the inlet and both cylinders were considered with zero gradients, and the prescribed pressure equal to zero was defined at the outlet (Fig. 2c, detail "O"). Finally, both upper and lower walls of the domain were set as slip condition (Fig. 2c, details "U" and "L", respectively). Transient numerical simulation was executed with a time step of 4×10^{-5} s, delimited by a Courant number lesser than 1. With this value, it is possible to compare the numerical results obtained with other experimental studies performed in the LMF, where the frequency acquisition of the experiments is usually 1×10^{-3} s. The convergence criterion for the residuals was set as 1×10^{-6} for the pressure and velocity field, and also for the turbulent kinetic energy.

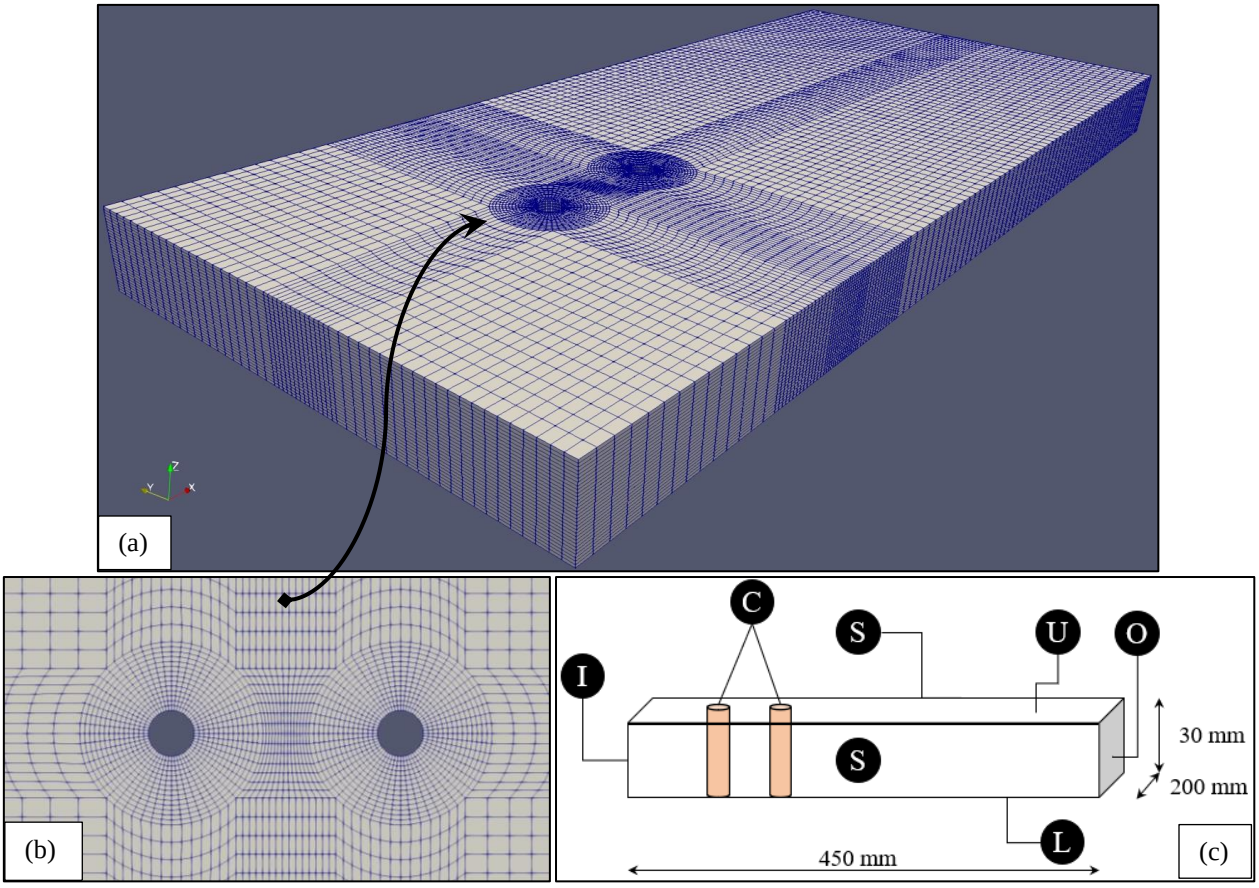

Figure 2. Isometric view of the mesh used in the present work (a), the mesh region close to the cylinders (b), and details of the boundary conditions (c).

3. RESULTS

3.1 Mesh quality analysis

To analyze the mesh quality of this study, the portion of the resolved turbulent kinetic energy by the mesh was compared with the total turbulent kinetic energy, as described by Eq. (3). In the present study, as there is an interest in the vortex structure region behind the cylinders, the mesh quality analysis occurred in three points behind the cylinder: the two tangent cylinder walls and the center of the cylinder. Thus, the k_{index} was computed in a line with 30 mm of length starting from these points, in both upstream and downstream cylinders, as shown in Fig. 3a and Fig. 3b, respectively. As the flow velocity and Reynolds number are the same for all the proposed spacing ratios, it was only presented the mesh analysis for the spacing ratio $T/D = 5$.

In Fig. 3a, the k_{index} of the upstream cylinder is presented for the three analyzed points. For the tangent cylinder wall points, the k_{index} starts from zero and achieves values above 0.8 at an axial distance of 0.004 m and remains in this condition as the flow is analyzed far from the cylinder walls. This behavior of the k_{index} shows that the flow is being modeled for the most part in the regions close to the cylinder walls. As the analyzed point moves away from the wall, the portion of the resolved turbulent kinetic energy is increased. Still, the point in the cylinder center presents the same behavior as the tangent cylinder wall points, but, in this case, values above 0.8 are obtained at a lesser distance, since in this region the flow velocity is lower than the other two points. In Fig. 3b, the same mesh quality analysis employed for the upstream cylinder (Fig. 3a) is adopted for the downstream cylinder. The points located in the two tangent cylinder

walls achieved values above 0.8 at an axial distance of 0.003 m, and the point at the cylinder center achieves this condition at 0.006 m. In the majority of the other regions of the mesh, values very close to 1 were found. Despite this, some points in the flow between the cylinders presented values of k_{index} ranging 0.65 – 0.75, i.e., were not able to achieve values above the intended value of 0.8. However, the authors chose to simulate with this condition and more comments about the mesh will be made in the next sections.

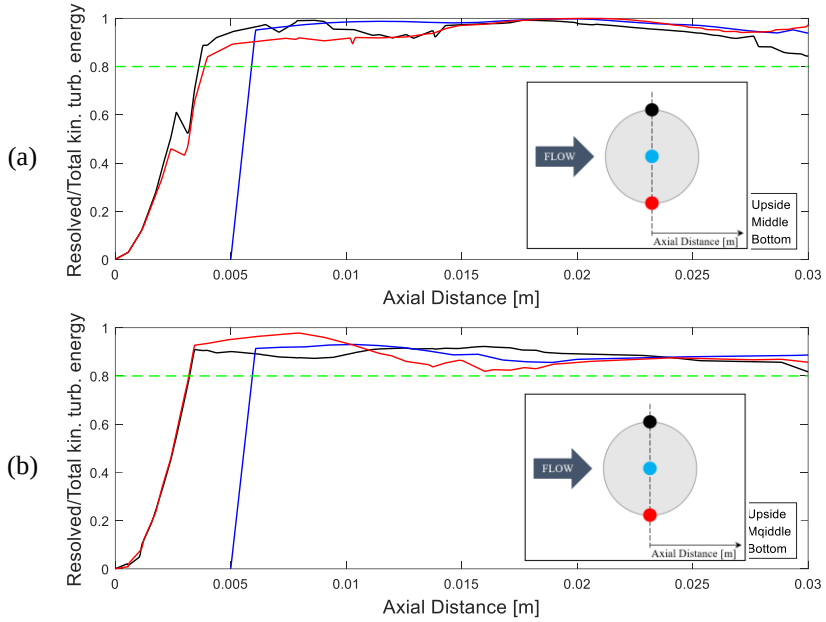

Figure 3. Mesh quality analysis for the upstream (a) and the downstream cylinder (b).

3.2 Force coefficients c_D and c_L

The results of drag and lift coefficients (c_D and c_L, respectively) for the present study are shown in Table 1-2 and Fig. 4. For $T/D = 5$, the time-averaged drag coefficients for the upstream and downstream cylinders are respectively 1.60 and 0.34 (Table 1). The second proposed T/D ratio of 7.5 presented time-averaged drag coefficients of 1.64 and 0.41 for upstream and downstream cylinders, respectively. References value of the time-averaged drag coefficients for these T/D ratios is 1.3 for the upstream cylinder and both T/D ratios, and 0.3 and 0.36 for the downstream cylinder for T/D ratios of 5 and 7.5, respectively (Alam et. al, 2003). This comparison shows good accordance for the c_D of the downstream cylinder and a small difference in the c_D of the upstream cylinder. For the last proposed T/D spacing ratio of 10, the time-averaged drag coefficients for the upstream and downstream cylinders are 1.67 and 0.98, respectively. In this case, it is expected that the cylinders have a behavior similar to a single cylinder. Finally, the time-averaged fluctuating drag coefficients ($c_D{}'$) were computed, and values of ~ 0.30 and ~ 0.3–0.37 were found for the upstream and downstream cylinders, respectively, considering all the T/D cases. Reference values for $c_D{}'$ are ~ 0.15 for the upstream cylinder, and ~ 0.23 for the downstream cylinder, considering a Reynolds number of 5.5×10^4 (Alam and Meyer, 2011).

Table 1. Time-averaged drag coefficients for the studied T/D ratios and both upstream and downstream cylinders.

	Time-averaged drag coefficient	
T/D ratio	Upstream Cylinder	Downstream Cylinder
5	1.60	0.34
7.5	1.64	0.41
10	1.67	0.98

Figure 4a-c presents the instantaneous lift coefficients computed for all the proposed T/D spacing ratios of 5, 7.5, and 10, respectively. The time-averaged lift coefficients extracted from Fig. 4a-c presented values close to zero in all the studied T/D ratios and both upstream and downstream cylinders, as expected (Assi, 2009). The time-averaged fluctuations of the lift coefficients ($c_L{}'$) of the upstream and downstream cylinders were computed using the RMS values (Root Mean Square) of the fluctuations presented in Fig. 4a-c, through the Matlab software, and these results are presented in Table 2. Reference values for $c_L{}'$ ranges of 0.5 for upstream cylinder and 0.6–0.73 for downstream cylinder in the T/D studied cases (Alam et al., 2003).

Table 2. Time-averaged fluctuations of lift coefficients for the studied T/D ratios and both cylinders.

	Time-averaged fluctuations of lift coefficients	
T/D ratio	Upstream Cylinder	Downstream Cylinder
5	0.85	1.06
7.5	0.87	0.55
10	0.86	1.18

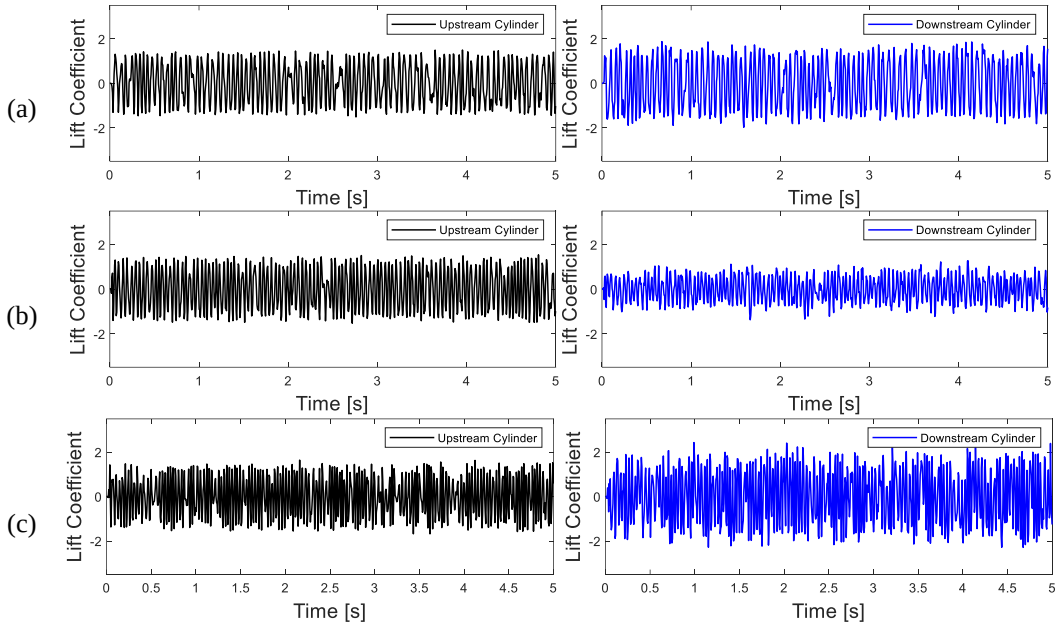

Figure 4. Instantaneous values of lift coefficients for upstream (left charts) and downstream (right charts) cylinders, for the T/D ratios of 5 (a), 7.5 (b), and 10 (c).

Some differences between the obtained force coefficients results in this work (Tables 1 and 2, Fig. 4a-c) and the reference values were found during these analyzes, mainly in the force coefficients of the upstream cylinders. The main reasons for these differences are: (a) the blockage ratio, in this work the blockage ratio was neglected since the experiments that will be performed has 1% of blockage ratio and the reference values are generally ranging from 8–12%; (b) Reynolds number and turbulence intensity, despite the proposed and the reference Reynolds numbers be in the same subcritical Reynolds range, particularly, the fluctuation force coefficients $c_D{}'$ and $c_L{}'$ presents strong dependence on the Reynolds number and turbulent intensity (Gartshore, 1984); (c) mesh quality, as already mentioned, the field of the k_{index} presented points of $k_{index} < 0.8$ that can affect the pressure field and lead to incorrect forces in the cylinders; (d) the boundary conditions on the upper and lower walls, that were set as slip condition in this work, and in experimental studies these walls have the no-slip condition. Future studies will evaluate the reasons.

3.3 Axial velocity signal (u) and Strouhal numbers

To obtain the velocity signal from the proposed cases, three probes were positioned in the flow domain, behind upstream and downstream cylinders. The probes were positioned 15 mm far from the center of the cylinder on the x-axis and tangent to the cylinder wall on the y-axis (Fig. 5). In the z-direction, the probes were distributed as follows: the probe 2 (P2) was located in the center of the cylinder, and probe 1 (P1) and probe 3 (P3) were inserted 10 mm far from the P2, P1 above, and P3 below the central probe P2, as presented in Fig. 5. These positions were adopted considering previous studies of Habowski et al. (2019) that positioned the probes in similar locations to identify the vortex shedding and compute the Strouhal numbers. Each probe calculates the flow velocity in the three-dimensional axis: x-, y-, and z-directions, corresponding to the velocity components u, v, and w, respectively. However, in the present work, due to reasons of space, only the axial velocity u will be discussed.

The velocity signals for the axial component on both upstream and downstream cylinders for the studied T/D spacing ratios are presented in Fig. 6a-c. Three velocity signals are presented in each chart of Fig. 6a-c, corresponding to the three positioned probes, as described in Fig. 5. Several velocity fluctuations are observed in all the charts of Fig. 6. A statistical analysis of these results is presented in Table 3, contemplating the mean results of the three probes for mean velocity, standard deviation, skewness, and kurtosis.

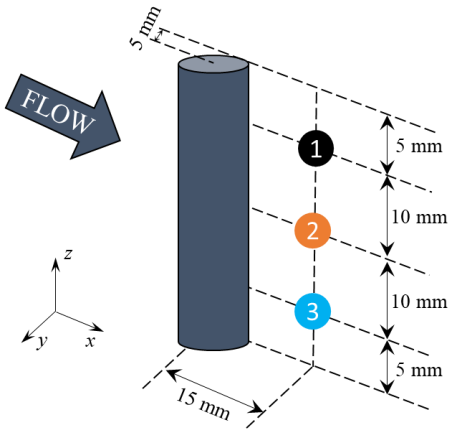

Figure 5. Scheme of the probe positions (P1 – black, P2 – orange, and P3 – blue) to obtain the velocity signals.

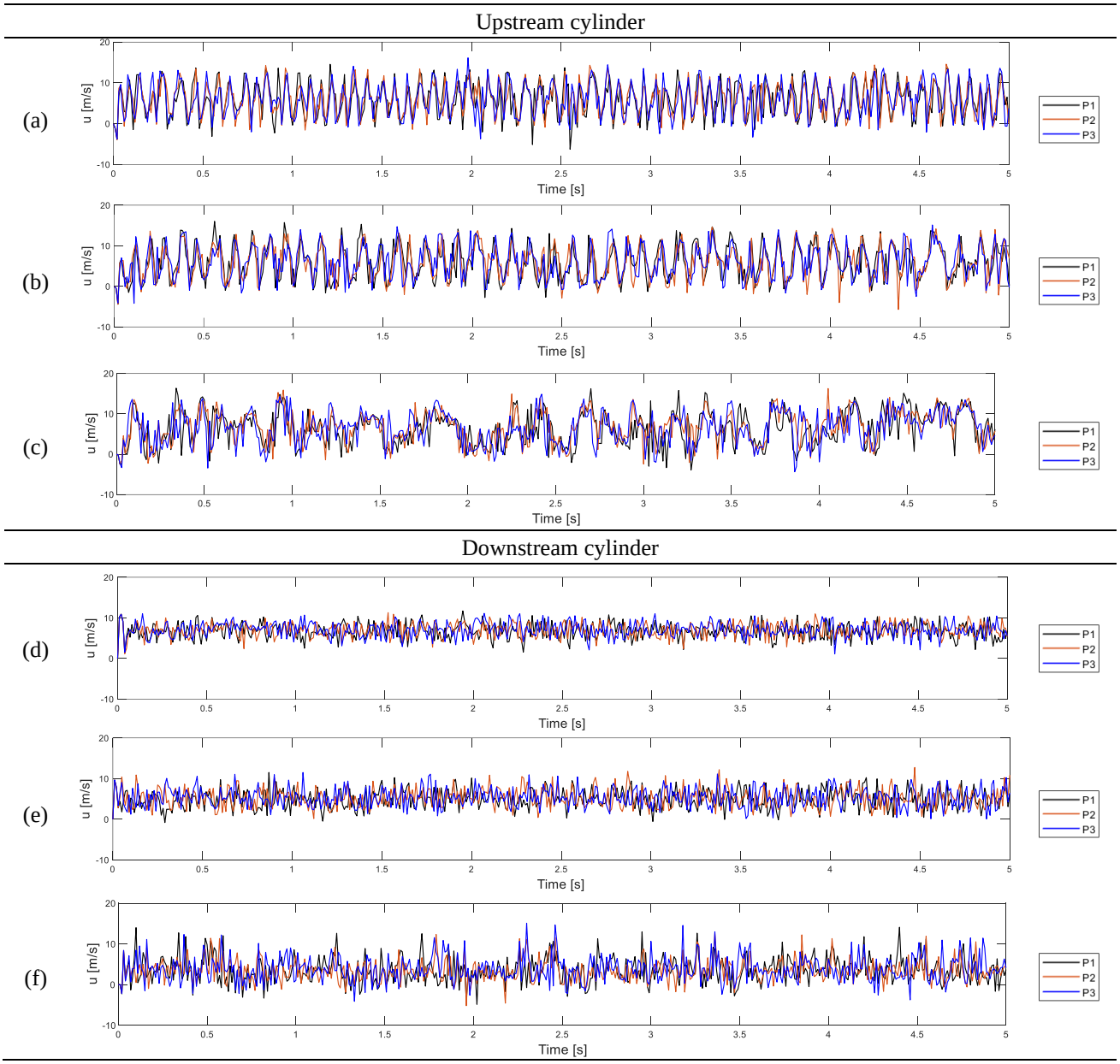

Figure 6. Axial velocities for the upstream cylinder and T/D spacing ratios of 5, 7.5, and 10 (a-c, respectively). Axial velocities for the downstream cylinder and T/D spacing ratios of 5, 7.5, and 10 (d-f, respectively).

Table 3. Statistical analysis for the velocity signals presented in Fig. 6.

	Upstream cylinder				Downstream cylinder			
T/D	Mean [m/s]	SD [m/s]	Skewness	Kurtosis	Mean [m/s]	SD [m/s]	Skewness	Kurtosis
5	5.950	4.077	-0.054	2.200	6.985	1.820	-0.227	3.282
7.5	6.203	4.068	-0.036	2.165	5.175	2.370	0.264	2.678
10	6.515	4.177	-0.026	2.177	3.724	2.933	0.586	3.768

Comparing the three probes of the upstream cylinder and $T/D = 5$ (Fig. 6a), the values of the velocity series are very similar, where a difference of 2.81% in its mean values was calculated. As the probes are close to each other, this behavior was expected, but for cylinders placed side-by-side in similar conditions, a different behavior is described by Neumeister et al. (2018), where the values of the axial velocity along the z-axis are very dependent of its z-axis position. High velocity fluctuations are observed (Fig. 6a) and also described in Table 3, where the fluctuations, shown by the standard deviation values, represent about 70% of the mean velocity value. The low value of skewness, close to zero, means that the signal is practically symmetric. The other velocity signals for the upstream cylinder, $T/D = 7.5$, and $T/D = 10$ (Fig. 6b and c, respectively), presented a very similar behavior as described for the case of $T/D = 5$, and also similar values for the statistical values analyzed (Tab. 3, second column). The values of the kurtosis for these three velocity signals (Fig. 6a-c) are very similar, showing that the tails in these velocity signals are similar. The presented analysis showed that the upstream cylinders of tandem arrangements do not present significant differences when the values of T/D spacing ratios are varied.

On the other hand, downstream cylinder results for the velocity signals present different behaviors when the three T/D studied cases are compared (Fig. 6d-e, third column of Tab. 3). It is clear that when the axial distance between the cylinders is increased, the mean velocity value behind the downstream cylinder is decreased while the velocity fluctuations in these same locations are increased. Despite this, these velocity signals (Fig. 6d-e) still present good symmetry and very similarity in the tails of the signal. Similar to the upstream cylinders, the three positioned probes presented similar behavior for each T/D studied in the downstream cylinders.

The Strouhal numbers of all the studied T/D spacing ratios were computed using the vortex shedding frequency from the velocity signals in Fig. 6. To obtain the vortex shedding frequencies, the Fourier analysis was applied to these signals, with the support of the Matlab software. Results for Strouhal numbers presented the same result of 0.195 for all the studied T/D ratios and both upstream and downstream cylinders, considering the free flow velocity (U) of 10 m/s and the cylinder diameter (D) of 10 mm. Results for the Strouhal number presented in the literature for similar experiments (Alam et al., 2003, and Alam and Meyer, 2011) show that the reference values are 0.195 and 0.2, for the upstream and downstream cylinder, respectively, presenting good accordance with the present work.

3.4 Flow visualization

A flow visualization qualitative analysis is proposed in the present study comparing the obtained velocity flow field for the T/D spacing ratios and the experimental flow visualization performed by Neumeister et al. (2022). Neumeister et al. (2022) explored flow visualization by colored water in a hydrodynamic channel for two circular tandem cylinders placed in T/D ranging from 2.5 to 10, and a Reynolds number of 2×10^3. A comparison for $T/D = 5$ is presented in Fig. 7.

Through the visual comparison of Fig. 7a-c, it is observed that the vortex shed from the upstream cylinder reattaches the downstream cylinder. This same result was already observed in other similar works (Alam et al., 2011), where the authors classified the vortex shedding and the reattachment as "co-shedding flow regime", and identified very high time-averaged fluctuating drag forces. Figure 7d shows that the vortex shed from the upstream cylinder influences the flow field between the cylinders and it is identified the reattachment of the shear layer. The flow field presented in this study with $T/D = 5$ (Fig. 7a-c) showed good agreement with both cited references (Alam et al., 2011; Neumeister et al., 2022).

The same qualitative analysis was performed for the other T/D spacing ratios, but the figures were not present here for reasons of space. For T/D spacing ratios of 7.5 and 10 were also observed the influence of the upstream vortex shedding in the flow field between both cylinders. However, it was observed that this influence is lesser when compared with $T/D = 5$, since the gap between the cylinders is higher and the vortex has more time and distance to dissipate its energy to the flow before achieving the downstream cylinder. Despite this, the reattachment of the shear layer into the downstream cylinder is still observed. Neumeister et al. (2022) emphasized that the transversal acceleration of the downstream cylinder in configurations with $T/D = 10$ is higher when compared with single cylinder transversal acceleration results, concluding the influence of the vortex shedding from the upstream cylinder.

4. FINAL REMARKS

This article presented the numerical study of a pair of circular cylinders tandem placed to a turbulent crossflow. Spacing ratios (T/D) of 5, 7.5, and 10 were computed using LES simulation with k-dynamic modeling for the turbulence.

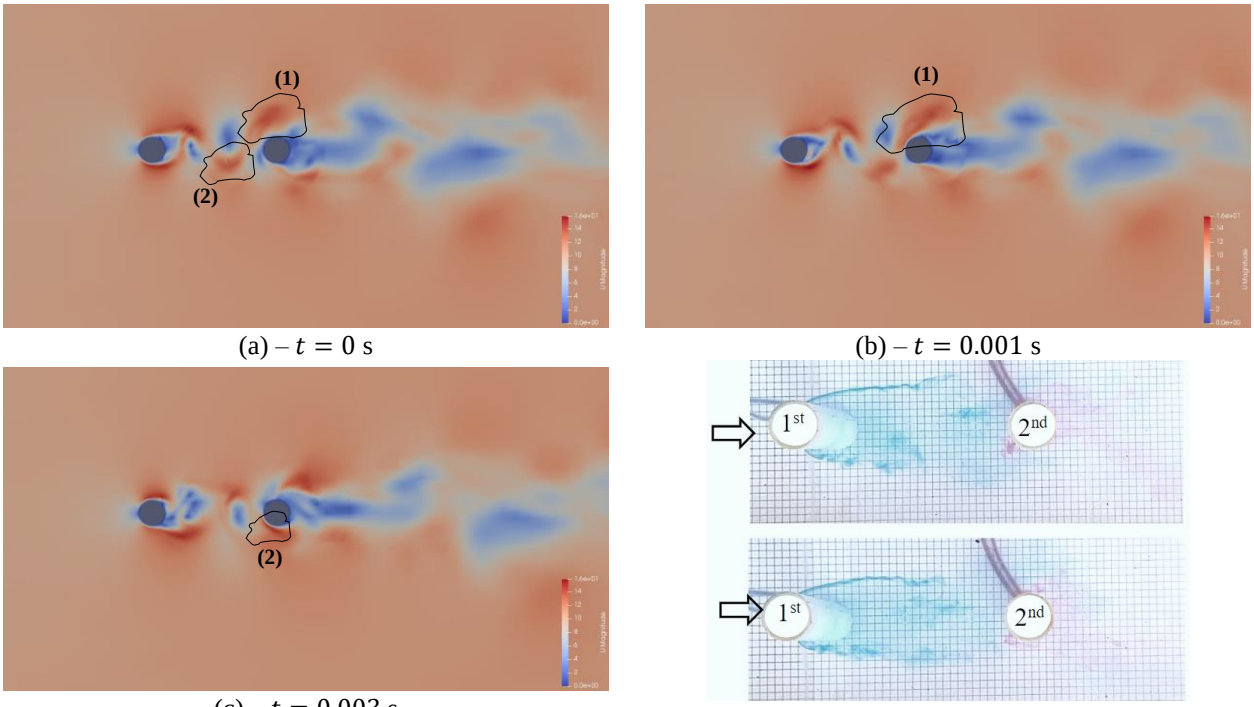

(a) – $t = 0$ s (b) – $t = 0.001$ s

(c) – $t = 0.003$ s (d) – Neumeister et al. (2022)

Figure 7. Comparison of velocity flow fields of the present study in time steps (a–c) and the experimental reference study of Neumeister et al. (2022) (d).

The simulations were performed by the OpenFOAM open-source software version 9, and the mesh was generated by the gmsh open-source software. The inlet turbulent flow was set with a velocity of 10 m/s and turbulence intensity of 1%, generating a Reynolds number of 6.67×10^3 computed for the cylinder diameter of 10 mm. Mesh quality analysis, force coefficients, velocity signal, Strouhal numbers, and flow visualization were obtained and compared with numerical and experimental results presented in the literature.

Results for lift and drag coefficients presented a good agreement with the literature for the downstream cylinder values of c_D, c_L and $c_L{}'$. For the upstream cylinder, small differences with the reference values were identified, mainly in the fluctuation Results. These disagreements could be caused by the coarse mesh in a few points, boundary conditions, the blockage ratio, Reynolds number, and the turbulence intensity level.

Velocity signal results showed that the axial velocity does not vary significantly along the z-axis for the considered probe distances. Comparing the flow velocity from the upstream and downstream cylinders it was identified that, as the T/D spacing ratio is increased, the mean flow velocity behind the downstream cylinder decreases while the velocity fluctuations are increased. In addition, all the analyzed velocity signals presented good symmetry. Strouhal numbers of 0.195 were computed for all the studied T/D spacing ratios and both upstream and downstream cylinders, considering the reference flow velocity of 10 m/s and the tube diameter of 10 mm, being in accordance with the reference values.

Finally, the flow visualization presented the vortex reattachment and the influence of the vortex shedding from the upstream cylinder into the downstream cylinder, as previously observed in other studies. In the largest $T/D = 10$ ratio in this study, the vortex reattachment was also observed.

Future studies contemplating a wide analysis of the mesh quality and experimental results in an aerodynamic channel with the same configurations for the flow and the cylinders setup are intended.

5. ACKNOWLEDGEMENTS

This study was financed in part by the Coordenação de Aperfeiçoamento de Pessoal de Nível Superior – Brasil (CAPES) - Finance Code 001.

6. REFERENCES

Alam, M.M., Moriya, M., Takai, K., and Sakamoto, H., 2003. “Fluctuating fluid forces acting on two circular cylinders in a tandem arrangement at a subcritical Reynolds number”. Journal of Wind Engineering and Industrial Aerodynamics, Vol. 91, pp. 139–154.

Alam, M.M. and Sakamoto, H., 2005. “Investigation of Strouhal frequencies of two staggered bluff bodies and detection of multistable flow by wavelets”. Journal of Fluids and Structures, Vol. 20, pp. 425–449.

Alam, M.M., and Meyer, J. P, 2011. “Two interacting cylinders in cross flow”. Physical Rev. E, Vol. 84, n. 5, 056304.

Assi, G.R.S, 2009. *Mechanisms for flow-induced vibration of interfering bluff bodies*. PhD thesis, University of London, Department of Aeronautics, London, United Kingdom.

Blevins, R.D., 1990. Flow-induced vibration. Van Nostrand Reinhold.

Derakhshandeh, J.F., Arjomandi, M., Dally, B., and Cazzolato, B., 2014. "The effect of arrangement of two circular cylinders on the maximum efficiency of Vortex-Induced Vibration power using a Scale-Adaptive Simulation model". Journal of Fluids and Structures, Vol. 49, pp. 654–666.

Gartshore, I.S., 1984. "Some effects of upstream turbulence on the unsteady lift forces imposed on prismatic two-dimensional bodies". ASME Journal of Fluids Eng., Vol. 106, pp. 418–424.

Habowski, P.B., Fiorot, G.H., de Paula, A.V. and Möller, S.V., 2020a. "Unbalanced free to oscillate tandem cylinders in a turbulent crossflow". Proceedings of the18th Brazilian Congress of Thermal Sciences and Engineering, Online.

Habowski, P.B., de Paula, A.V. and Möller, S.V., 2020b. "Wake behavior analysis for two circular cylinders placed at several angles to the flow". Journal of the Brazilian Society of Mechanical Sciences and Engineering, Vol. 42.

Habowski, P.B., de Paula, A.V. and Möller, S.V., 2019. "Analysis of the wake of two parallel circular cylinders at several angular positions to the flow". Proceedings of the COBEM 2019 - 25th International Congress of Mechanical Engineering. Uberlândia, MG - Brasil.

Habowski, P.B., Neumeister, R.F., de Paula, A.V., Petry, A.P. and Möller, S.V., 2022. "On the interaction of the wake flow with the rotation process of two parallel free-to-rotate cylinders submitted to an accelerating flow". Acta Mechanica, Vol. 233, pp. 813–835.

Igarashi, T., 1981. "Characteristics of the flow around two circular cylinders arranged in tandem (first report)". Bulletin of JSME, Vol. 24, pp. 323–331.

Kim, S., Alam, M.M., Sakamoto, H. and Zhou, Y., 2009. "Flow-induced vibrations of two circular cylinders in tandem arrangement. part 1: Characteristics of vibration". Journal of Wind Eng. and Ind. Aerod., Vol. 97, pp. 304–311.

Kim, W.W. and Menon, S., 1995. "A new dynamic one-equation sub-grid scale model for large eddy simulations". American Institute of Aeronautics and Astronautics Inc, AIAA.

McDermott, R.J., Forney, G.P., McGrattan, K., and Mell, W.E., 2010. "Fire Dynamics Simulator 6: Complex Geometry, Embedded Meshes, and Quality Assessment". Proceedings of the V European Conference on Computational Fluid Dynamics, Lisbon, Portugal.

Neto, A.S., 2002. "Simulação de grandes escalas de escoamentos turbulentos". In Turbulência, ABCM, Rio de Janeiro RJ, Brazil, chapter 4, pp. 159–190.

Neumeister, R.F., Ost, A.P., Habowski, P.B., de Paula, A.V., Petry, A.P., and Möller, S.V., 2022. "Wake induced vibration in tandem cylinders: Part 1 – Wake perturbation analysis". Proceedings of the 12th International Conference on Flow-Induced Vibration, pp. 103–110, Paris-Saclay, France. Available in: https://fiv2020.sciencesconf.org/resource/page/id/22.

Neumeister, R.F., Petry, A.P., and Möller, S.V., 2018. "Characteristics of the wake formation and force distribution of the bistable flow on two cylinders side-by-side". Journal of the Brazilian Society of Mechanical Sciences and Engineering, Vol. 40, pp. 1–19.

Neumeister, R.F., Petry, A.P. and Möller, S.V., 2021. "Experimental flow-induced vibration analysis of the crossflow past a single cylinder and pairs of cylinders in tandem and side-by-side". Journal of Pressure Vessel Technology, Transactions of the ASME, Vol. 143, pp. 1–13.

Palau-Salvador, G., Stoesser, T., and Rodi, W., 2008. "LES of the flow around two cylinders in tandem". Journal of Fluids and Structures, Vol. 24, pp. 1304–1312.

Pope, S.B., 2004. "Ten questions concerning the large-eddy simulation of turbulent flows". New Journal of Physics, Vol. 6, n. 35, pp. 1–24.

Sumner, D., 2010. "Two circular cylinders in cross-flow: A review". Journal of Fluids and Structures, Vol. 26, pp. 849–899.

Sumner, D., Price, S.J. and Païdoussis, M.P., 2000. "Flow-pattern identification for two staggered circular cylinders in cross-flow". Journal of Fluid Mechanics, Vol. 411, pp. 263–303.

Wilcox, D., 2006. Turbulence Modeling for CFD. DCW Industries, California, 3rd edition.

Yao, W. and Jaiman, R.K., 2019. "Stability analysis of the wake-induced vibration of tandem circular and square cylinders". Nonlinear Dynamics, Vol. 95, pp. 13–28.

Zdravkovich, M.M., 1987. "The effects of interference between circular cylinders in cross flow†". Journal of Fluids and Structures, Vol. 1, pp. 239–261.

Zhao, R., Xu, J-L., Yan, C., and Yu, J., 2011. "Scale-adaptive simulation of flow past wavy cylinders at a subcritical Reynolds number". Acta Mechanica Sinica, Vol. 27, pp. 660–667.

Zhou, Y. and Alam, M.M., 2016. "Wake of two interacting circular cylinders: A review". International Journal of Heat and Fluid Flow, Vol. 62, pp. 510–537.

7. NOTICE

The authors are solely responsible for the printed material included in this paper.